

Interpretative model of standard stationary wavefunctions in 1D closed motions context

GIUSEPPE MASTROCINQUE

Dipartimento di Scienze Fisiche
dell'Università di Napoli "Federico II"
Facoltà di Ingegneria - P.le Tecchio - 80125 Napoli
email: mastroci@unina.it

ABSTRACT. A particular development for the one dimensional oscillator stationary wavefunctions is investigated. Going from the real space to the complex, the periodicity condition requires that the wave phase is a sum of Heaviside functions, and the phase gradient the corresponding sum of DiracDeltas. This implies a violation of the linearity, although restrained to a space with null extension. On one hand, this leaves unchanged, to all practical effects, the ordinary description based on the linear wave equation. But on the other, it allows us to set up a bridge with a non-linear model we have developed in previous papers. In this last, the phase gradient is distributed along the available space while in the former, it concentrates in the wavefunction knots. In this way, it is possible to import the non linear model equations (and interpretation) into the standard quantum mechanics framework. So we set up a model (SQM⁺) which keeps exactly the same expressions for the wavefunctions as given by standard quantum mechanics; but with added values, only placed in the knots, of generalised functions. As a result, we become able to solve in the non linear domain, which implies some peculiar constraints. These last are properties of the energy and mass fluctuations characterising the model, and giving it the name. In this way, we calculate the Newtonian-like microcanonical ensemble subtending, by the fluctuation model interpretation, the standard quantum mechanical wavefunctions.

RÉSUMÉ. Nous étudions un développement particulier de la fonction d'onde stationnaire d'oscillateur à une dimension. En passant de l'espace réel au complexe, la condition de périodicité de l'onde nous oblige à considérer la phase comme somme de fonctions d'Heaviside, et son gradient comme somme de fonctions Delta de Dirac. Il s'ensuit une violation de la linéarité, se restreignant par ailleurs à un domaine d'extension nulle. D'une part alors, cela laisse inchangée, à tout effet pratique, la description ordinaire fondée sur l'équation d'onde linéaire. Mais de l'autre, ça nous permet de bâtir un pont avec un modèle non-linéaire que nous avons introduit dans des travaux précédents. Dans

ce dernier, le gradient de phase est distribué dans l'espace tandis que dans l'autre, ils se concentrent dans les nœuds de la fonction d'onde ordinaire. Il est alors possible d'importer les équations (et l'interprétation) du modèle non linéaire dans le cadre de la mécanique quantique standard. On a donc développé un modèle (SQM^+) qui garde exactement les mêmes expressions pour les fonctions d'onde, données par la mécanique quantique ordinaire ; mais elles y sont ajoutées, dans les nœuds seulement, des valeurs généralisées. De cette façon, on peut résoudre dans le domaine non linéaire, qui pose des contraintes particulières. Ces contraintes sont des propriétés des fluctuations d'énergie et de masse qui donnent le nom au modèle. On peut ainsi calculer l'ensemble microcanonique à caractère Newtonien sous-tendant les fonctions d'onde standard, selon l'interprétation du modèle des fluctuations.

PACS. 45.50.-j - Dynamics and kinematics of a particle and a system of particles. PACS. 03.65.Ta - Foundations of Quantum Mechanics

1 Introduction

In a few previous papers [1,2] we introduced a classical-like model for the oscillators dynamics, able to account for (peculiarly defined) energy and mass fluctuations. It seems to us fit to solve some basic incongruences between classical and quantum theories. The model rests a) on a classical dynamics part, including the variable mass concept and typical potential energy functions ; and b) on a quantum part, based on a non linear wave equation with a variable density current (in contrast with the corresponding, standard quantum mechanical stationary case). The variable current is correlated with both the energy and mass fluctuations. The simplest view about the new model is through the ordinary fluid-dynamic (Madelung-like) approach ; but the (non standard) wave phase gradient $\nabla S/\hbar$ is now defined, as in a typical non linear wave coupling, by the difference of two other characteristic wave vectors. The positional densities solving the non linear wave equation come out very similar to the known quantum ones, with one difference : they show minima, instead of zeros in the nodes. The entire framework is shown to be consistent with the basic features of both classical and quantum mechanics. So these last are brought to some reconciliation, at least in the stationary, 1D, spinless case by now. Within the quoted limits, the model can also be considered as an extension of the de Broglie-Bohm mechanics accounting for energy broadening and mass fluctuations. By the way, it should be noted that many experiments in recent years, pointing at the physics of

the so called walking, orbiting, or bouncing droplets [4 ÷ 10], have provided extraordinary conceptual support for a renovated interpretation of quantum mechanical effects by the pilot-wave-like theories.

So the new model is based on a non linear (NL) wave equation. Developments are still wanted ; but since now, we can start with investigating its relationships with the standard quantum mechanics (SQM) - this last is based instead on the linear postulate. So we can look at the SQM ⁽¹⁾ role in the new model as the "linear approximation" of it. At least : limiting to a first glance, and just staying on a basic ground. Actually we have an interesting result to show here : the known SQM stationary wavefunctions seem to find a particular place in the new model. In the spirit of this last therefore, we will be able to find out in this paper the classical ensembles corresponding to the SQM densities (by these last, we intend precisely the standard solutions of the linear Schrödinger equation, in the stationary, uni-dimensional, closed motions case to which we limit ourselves at present).

2 Non linear model equations

Although the next equations have already been given in previous references, to our purposes we have to resume them briefly. We can write the NL wave equation for the stationary, 1D case as follows ($\Psi(x) \equiv$ wavefunction, $\Phi(x) \equiv$ potential energy, $\partial/\partial t = 0$, $' \equiv d/dx$, etc. as well known) :

$$\Phi(x) + i\Phi_{im}(x) - \frac{\hbar^2}{2m} \frac{\Psi(x)''}{\Psi(x)} = E^* \quad (1)$$

$$\Phi_{im}(x) = \frac{\hbar}{2\rho(x)} \frac{d}{dx} J(x) \quad (2)$$

The potential $\Phi_{im}(x)$ has been introduced in [1]. We name as usual $J(x)$ the density current, i.e. the quantity $\rho(x)\nabla S(x)/m$ ($S(x)/\hbar \equiv$ phase, $\rho(x) \equiv$ num. density) ; but in eq. (2) non-standard values (notably, x-dependent) of it are allowed. Obviously J can also be set equal to the standard value (a constant J_0 in the stationary case) : then we recover

¹For brevity, we use the acronym SQM. Obviously, a precise definition of "standard quantum mechanics" could hardly be given here on general grounds. We use the locution essentially to indicate that body of knowledges reporting to the basic(non relativistic) linear wave equation and to the so called orthodox interpretation by the Copenhagen school.

the SQM equation. So including the last one, we will generally be able to describe all the cases throughout our papers, simply specifying an expression of $J(x)$. Using a Madelung formalism we can write (1) and (2) also in the form :

$$\Psi(x) = \sqrt{\rho(x)} \exp(iS(x)/\hbar) \quad (3)$$

$$\frac{\nabla S^2(x)}{2m} + \Phi(x) - \frac{\hbar^2}{2m} \frac{\sqrt{\rho(x)''}}{\sqrt{\rho(x)}} = E^* = E_n \quad (4)$$

$$\frac{\rho(x)\nabla S(x)}{m} = J(x) \quad (5)$$

Here we have only the x axis so that ∇ means $\nabla_x \equiv d/dx$ (2). As is usual, we will call "Bohm potential" the quantity

$$\Phi_B(x) = - \frac{\hbar^2}{2m} \frac{\sqrt{\rho(x)''}}{\sqrt{\rho(x)}} \quad (6)$$

In case of closed motion, the energy E^* is a standard eigenvalue of the potential and we have set $E^* = E_n$ to mean the n th state energy. The density current being a constant J_0 in stationary SQM, in order to report to this case we will write specifically

$$\nabla S_{sqm}(x) = m \frac{J_0}{\rho_{qm}(x)} \quad (7)$$

Note that in Bohm mechanics, ∇S_{sqm} is identified with the (classical-like) momentum

$$\nabla S_{sqm}(x) \equiv m v_D(x) \quad (8)$$

where $v_D(x)$ is the implicated Eulerian velocity field. This quantity is generally intended as the velocity of an "equivalent" particle or, better expressed, a packet group velocity. In our model instead, we define $\nabla S(x)$ as

$$\nabla S(x) = m \frac{J(x)}{\rho(x)} = m_{eff}(x) v_D(x) - \frac{c_n \hbar \nu(x)}{2v_D(x)} \quad (9)$$

$$\oint \nabla S(x) dx = (n-1) \hbar \quad (10)$$

²Yet for brevity in our papers, we use the notation $\nabla S(x)$ in the sense of its absolute value. When the sign is important, we write $\nabla_x S(x)$, as f.i. in eqs. (27) and (28).

$$v_D(x) = n_B \frac{\nu(x)}{\rho(x)} \quad (11)$$

So the current $J(x)$ in (9) is variable in space, according to the behaviour of the various quantities there involved. We have named $m_{eff}(x)$ the variable mass function and $\nu(x)$ the particles (numerical) flow along the x-axis. To us, $v_D(x)$ still is an "equivalent", or "group", velocity - it does not take, on a general plane, a different interpretation from Bohm's one; but we believe it can be better appreciated in the new context ⁽³⁾. Specifically, eq. (11) correlates $v_D(x)$ to n_B - this is the number of distinguishable beams of particles, that we consider to be present in the same space at once. In this paper, we will always have $n_B = 2$ because the density accounts for both the forward and backward beams of particles circulating in the oscillator space. The quantity

$$\Delta E(x) = c_n h \nu(x) \quad (12)$$

is the energy broadening or the fluctuation energy interval affecting the system. The simple assumption here is that the broadening is proportional to the particles flow in the beam. The coefficient c_n ⁽⁴⁾ depends on the ensemble of physical constraints imposed to the system; then it must be determined as an appropriate numerical value for each case at hand. The stronger the cause of the fluctuations, the greater will be this value. However on a general ground, we do not expect values much greater than unity in our stationary context. Smaller values may be instead considered, and even zeros when we want to push our model towards the limiting case of null fluctuations.

To the previous equations we add the normalisation equations (assume a symmetric potential around $x=0$; the points $\pm x_0^*$ stand for the extreme boundaries of space attainable by the oscillator)

$$\int_{-x_0^*}^{x_0^*} \rho(x) dx = 1 \quad (13)$$

$$\int_{-x_0^*}^{x_0^*} m_{eff}(x) \rho(x) dx = m \quad (14)$$

We consider this last condition the simplest and appropriate to express mass conservation as expected in a stationary situation; obviously,

³Note f.i. the properties in the next eqs. (60)÷(62), with related comments.

⁴The index n in it refers to the n th state of motion of the oscillator in closed space.

in the limit where mass fluctuations are neglected, it is always satisfied because of (13). For the sake of clarity, let us introduce here the quantity, which we name the effective mass density :

$$\rho_m(\mathbf{x}) = m_{eff}(\mathbf{x})\rho(\mathbf{x}) \quad (15)$$

Integrating this over a space domain X , we will get the mass statistically included in that domain. Then eq. (14) can be better expressed as

$$\int_{-x_0^*}^{x_0^*} \rho_m(\mathbf{x})d\mathbf{x} = m \quad (16)$$

We can say that statistically (per unit particle), the mass included in the oscillator space must turn out equal to m .

In order to solve the previous set of equations we need finally an expression for the effective mass (the *mass eigenfunction*), which we have determined in previous references as :

$$m_{eff}(\mathbf{x}, \text{II}) = \frac{c_n \hbar \rho(\mathbf{x})^2}{8\nu(\mathbf{x})} \quad (17)$$

in the region of space (named Reg. II in [1]) where $\nabla S(\mathbf{x}) = 0$; and

$$m_{eff}(\mathbf{x}, \text{I}) = m_{eff}(\mathbf{x}_n)g(\mathbf{x}) + \text{sign}(\rho'(\mathbf{x}))\rho'(\mathbf{x})^2\sigma_n |1 - c_n| \quad (18)$$

in the region of space (named Reg. I) where $\nabla S(\mathbf{x}) \neq 0$.

For more details than given here to the entire subject, one can also refer to [3] where a few *errata* on previous work are also given (not more than small errors in calculating some coefficients). Here we have to note that in the previous nomenclature, Region I of space is characterised by $\nabla S(\mathbf{x}) \neq 0$ and constant flow $\nu(\mathbf{x}) = \nu_{n0}$ at the same time. But in the present paper, we will be brought to consider a new region of space, where we will find at the same time $\nabla S(\mathbf{x}) = 0$ and $\nu(\mathbf{x}) = \nu_{n0}$. So to be clear, we have in the sequel of our paper 3 space regions. Since now, they define as follows : Reg. I, where $\nabla S(\mathbf{x}) \neq 0$, $\nu(\mathbf{x}) = \nu_{n0}$; Reg. II_a, where $\nabla S(\mathbf{x}) = 0$, $\nu(\mathbf{x}) = \nu_{n0}$; Reg. II_b, where $\nabla S(\mathbf{x}) = 0$, $\nu'(\mathbf{x}) \neq 0$. When calling at Reg. II, the ensemble of Reg. II_a and Reg. II_b must be understood. Region II_b is the boundary region of space where exhausted particles start with finding reflection at turning points, and coincides with the so-called evanescence region, where the quantum wave also takes a null wave vector $\nabla S(\mathbf{x}) = 0$.

We want now to discuss the relationship between our equations and the SQM apparatus. To this purpose, we have to calculate the limit of eqs. (4), (5) at constant current J_0 as a premise.

3 The linear approximation and SQM

Looking at eqs. (1)÷(5), we see that the linear Schrödinger equation is recovered from them when $J(x) \rightarrow J_0$. In this mathematical sense, we speak easily of a linear approximation stemming from our model; but the conceptual implications of this path are a wide domain to explore. In the following, we will investigate only the case $J_0 = 0$ which is of interest in this paper.

Taking $J(x) = 0$ implies $\nabla S = 0$ and brings the known standard (real) eigenfunctions into equations (1)÷(5) :

$$\Psi(x) |_{J_0=0} = \Psi_{qm}(x, n) \quad (19)$$

For the sakes of both concept and nomenclature, we refer to the Harmonic Oscillator example :

$$\Psi_{qm}^{HO}(x, n) = a_n \text{Exp}\left[-\frac{x^2}{2\lambda^2}\right] \text{HermiteH}\left[n - 1, \frac{x}{\lambda}\right] \quad (20)$$

Here a_n is a norm coefficient and λ is

$$\lambda = \sqrt{\frac{\hbar}{4\pi^2 m \nu_c}} \quad (21)$$

Fig.1 shows f.i. this wavefunction for the case $n = 4$ (arbitrary vertical scale). Note that by the Born postulate, we will also write in general

$$\Psi_{qm}(x, n) = \pm |\Psi_{qm}(x, n)| = \pm \sqrt{\rho_{qm}(x)} \quad (22)$$

so that $\rho_{qm}(x)$ is the SQM density, that we assume normalised as ($x_0^* \rightarrow \infty$ for HO) :

$$\int_{-\infty}^{\infty} \rho_{qm}(x, n) dx = 1 \quad (23)$$

By these steps, however, the relationship of our model with SQM is not fully exhausted - due to eq. (10). This is because we have taken travelling

waves as the fundamental basis in our model. To comply with (10), we have to introduce a phase, say

$$\phi(x) = \frac{S(x)}{\hbar} \quad (24)$$

So we ask that $\Psi_{qm}(x, n)$ is resolved into travelling components. It "seems well" therefore, that we can write (we are here in a SQM frame, use the linear superposition postulate) :

$$\Psi_{qm}(x, n) = \frac{1}{2} \sqrt{\rho_{qm}(x)} \left(\text{Exp}\left[i \frac{S(x)}{\hbar}\right] + \text{Exp}\left[-i \frac{S(x)}{\hbar}\right] \right) \quad (25)$$

Since we keep $\Psi_{qm}(x, n)$ as a real quantity, $\phi(x)$ must always be equal to some $p \pi$ with $|p|$ an integer, and we should also be allowed to write ⁽⁵⁾

$$\Psi_{qm}(x, n) = \sqrt{\rho_{qm}(x)} \text{Cos}\left[\frac{S(x)}{\hbar}\right] = \sqrt{\rho_{qm}(x)} \text{Exp}\left[i \frac{S(x)}{\hbar}\right] \quad (26)$$

Actually the phase $\phi(x)$ comes out as a multiple step function as shown f.i. in *Fig. 2* (for HO, $n = 4$). During its round trip, $S(x)$ adds a $\pi \hbar$ at each knot that is met with, where $\Psi_{qm}(x, n)$ changes sign. So, moving f.i. from $-\infty$ to $+\infty$ ⁽⁶⁾, we find at rigour ($f = forwards$, $b = backwards$) :

$$\begin{aligned} \nabla_x S_b(x) &= \pi \hbar \sum_{i=1}^{N_{knots}/2} \text{DiracDelta}[x-x_i] \\ &\equiv \pi \hbar \sum_{i=1}^{N_{knots}/2} \uparrow_i \{\text{wave travelling backwards, blue line}\} \end{aligned} \quad (27)$$

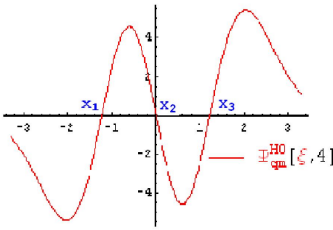
⁵When we use $\Psi_{qm}(x, n)$, $\rho_{qm}(x)$, $\nabla S_{qm}(x)$ etc. we may always keep in mind the HO example but we have turned out to the general case.

⁶Referring to *Fig. 2*, we have chosen forward motion from ∞ to $-\infty$ (red line), and backward vice-versa (blue). We name x_i the position of the i th wave knot. We have found useful starting with a phase = 0 in $-\infty$, so we count knots from 1 to $N_{knots}/2$ along the direction of backward motion. Turning back to the forward, we keep counting the knots again, so each zero is counted twice and N_{knots} is always an even number. With these choices, the backward and the forward phase functions are opposite in sign to each other (the same occurs to their gradients in x). Therefore in next equations, we can run i only from 1 to $N_{knots}/2$, knowing that changing versus to the motion merely implies a change of sign in the phase. This is the reason of the \pm sign we find in next eq. (32).

With $N_{knots} = 0$, $\nabla S(x) = 0$ is understood. For $n = 4$, $N_{knots} = 6$ and we show the positions x_1 , x_2 , x_3 in the example of *Fig. 1*. Sometimes it be easy, we may represent a Delta function with a vertical arrow at the right place.

$$\begin{aligned}
 \nabla_x S_f(x) &= -\nabla_x S_b(x) = -\pi \hbar \sum_{i=1}^{N_{knots}/2} DiracDelta[x-x_i] \\
 &\equiv \pi \hbar \sum_{i=1}^{N_{knots}/2} \downarrow_i \{ \text{wave travelling forwards, red line} \}
 \end{aligned}
 \tag{28}$$

Standard wavefunction of the Harmonic Oscillator, n = 4



Phase diagram for the Harmonic Oscillator, n = 4

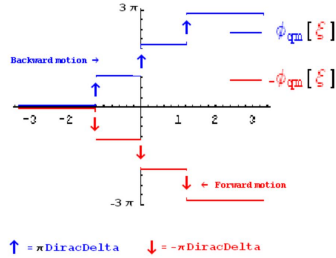


Fig.1- HO SQM wavefunction, n = 4 Fig.2- HO phase for travelling waves, n = 4

By equation (27), summing now over space (and accounting for all knots in the round trip), we find eq. (10) finally satisfied. We obviously have taken the area of each *DiracDelta* equal to 1. In all knots, we also find $J_0 = \rho_{qm}(x_i) \nabla S(x_i) = 0$, because

$$\rho_{qm}(x_i) = 0
 \tag{29}$$

Yet hidden in the previous equations, there is a bug. The Madelung form in standard quantum mechanics with (29) and an appropriate ∇S_{qm} should read

$$-\frac{\hbar^2}{2m} \frac{\Psi_{qm}(x, n)''}{\Psi_{qm}(x, n)} = \frac{\nabla S_{qm}^2(x)}{2m} - \frac{\hbar^2}{2m} \frac{\sqrt{\rho_{qm}(x)}''}{\sqrt{\rho_{qm}(x)}} = E_n - \Phi(x)
 \tag{30}$$

This shows us that that the expansion (25) with $\nabla S(x)$ taken as in (27), (28) is not supported by the standard Schrödinger equation - obviously, we refer to the knots. Indeed the terms $\nabla S^2(x_i)$ that we have assumed as consequent to the superposition principle, are "infinite". So they would stay unbalanced in eq. (30), because the standard Bohm potential is on the contrary, finite and continuous everywhere. The quantum mechanical eq. (30) with real $\Psi_{qm}(x, n)$ works well - provided $\nabla S_{qm}(x)$

is 0 everywhere. This breaks off with the superposition postulate in the complex plane.

To find support in this matter, we can help with our non linear model. Let us show how.

In each knot, the phase $\phi_{qm}^+(x)$ is not determined; taking the blue line as reference, it lies between $(i-1)\pi$ and $i\pi$. Let us ask for it to be definite, instead. By symmetry, its value can be set equal to

$$\phi_{qm}^+(x_i) = \left(i - \frac{1}{2}\right) \pi \quad (31)$$

This leads us to introduce the complex wavefunctions (let the Ψ_i^+ be real, positive quantities) in the form

$$\begin{aligned} \Psi_{qm}^+(x, n) &= \sqrt{\rho_{qm}^+(x)} \text{Exp}\left[i \frac{S_{qm}^+(x)}{\hbar}\right] = \\ &= \Psi_{qm}(x, n) \pm i \sum_{i=1}^{N_{knots}/2} \Psi_i^+ \text{DiscreteDelta}[x - x_i] \end{aligned} \quad (32)$$

$$\rho_{qm}^+(x, n) = |\Psi_{qm}^+(x, n)|^2 = \rho_{qm}(x, n) + \sum_{i=1}^{N_{knots}/2} \rho_i^+ \text{DiscreteDelta}[x - x_i] \quad (33)$$

$$\rho_i^+ = \Psi_i^{+2} \neq 0 \quad (34)$$

These (+)-marked functions are equal to the standard ones everywhere, except in the very knots positions where they take finite values. This is in agreement with the previous requirements on the phase. Note that $\Psi_{qm}^+(x, n)$ is *twice valued* by the \pm sign inside : it is a travelling wave, taking the sign + for the backward motion (then we find the phase in the knot $\phi_{qm}^+(x_i) = \text{ArcTan}(\infty) + (i-1)\pi$), and viceversa. So interestingly, eq. (26) sets the *full* wave in the form of 1 travelling wave, going back and forth : in agreement with nomenclature in *Fig.2*, when it goes forward, $S_{qm}^+(x)/\hbar = -\phi_{qm}^+(x)$ (red line); when it goes backward, $S_{qm}^+(x)/\hbar = \phi_{qm}^+(x)$ (blue line). So we could say, we have introduced some kind of *circular* wave : it is simply the *suite* (not the sum!) of the forward and backward waves; it spans the round trip in the oscillator's space just in the same way a classical particle goes back and forth. By construction, in each of the \pm waves quantum interference is accounted for already, since

their amplitude is twice the one dictated by the expansion (25). In this way, we have no need any more, to deal with 2 interfering waves as in (25). This is just a character of the non linear model we expounded in [1], too. The conceptual view inside, is that one can separate the interfering waves of quantum mechanics in 2 single waves, each of them bringing the right character for a good description. This corresponds to a model where each single wave does not interact directly with the other, but interacts with the "vacuum" being the intermediary between them. Supposedly, the vacuum "feels" both waves and consequent to that, reacts on them both; on account of all of this, we assume finally the forms (32), (33). Such a view will also allow us to set up a NL model of the tunnel effect, to come in a next article.

Reading all of this in the light of the model with variable current, we have not to comply with the constraint $J_0 = 0$ any more; but with eq. (9). The last will be worked out next; note here that eq. (4) in the knots can now be read

$$\frac{\nabla S_{qm}^{+2}(x_i)}{\hbar^2} = \frac{\sqrt{\rho_{qm}^+(x)} \Big|_{x \rightarrow x_i}}{\sqrt{\rho_i^+}} = \pi^2 DiracDelta[0]^2 \equiv \infty \quad (35)$$

The other terms are indeed negligible, being finite. For congruence therefore, we have set $\sqrt{\rho_{qm}^+(x)} \Big|_{x_i}$ as an infinite of the displayed form. Clearly, we are now using *generalised* functions everywhere, in the sense of Schwartz's distributions theory. We also have now (abs values intended)

$$J_{qm}^+(x) = \frac{\rho_{qm}^+(x, n) \nabla S_{qm}^+(x)}{m} = \frac{\hbar \pi \rho_{qm}^+(x, n)}{m} \sum_{i=1}^{N_{knots}/2} DiracDelta[x-x_i] \quad (36)$$

so that, in the knots

$$J_{qm}^+(x_i) = \frac{\rho_i^+ \nabla S_{qm}^+(x_i)}{m} = \frac{\hbar \rho_i^+ \pi}{m} DiracDelta[0] \equiv \infty \quad (37)$$

Thus when we take the limit $J_0 \rightarrow 0$ this cannot be kept everywhere if we want eq. (10) satisfied. In the knots, J_0 has to stay as a Dirac Delta while it is zero elsewhere. So turning to the SQM frame, we have shown this: if we believe that a travelling wave expansion as in (25) should be feasible,

a variable current density must be introduced into stationary quantum mechanics. This breaks off with linearity. However, it is clear that since the Lebesgue extension of the relevant domain for Delta functions is zero, and moreover the area of a DiscreteDelta is zero, for practical purposes in the SQM context the new wavefunctions $\Psi_{qm}^+(\mathbf{x}, n)$ given here are not distinguishable from the standard ones. Even normalisation of the density is unchanged. So it may be concluded.. that the SQM formalism is practically unaffected by these subtilities.

The same subtilities, however, will allow us to conceive a classical-like interpretation just for the SQM wavefunctions and related framework. This is reserved to the next section. Here note first, that the "extended" functions (32) and (33), together with (35), bring into quantum mechanics still a couple of characters more, that we have found in the non linear model already : 1) nowhere the wave amplitude and density become "exactly zero" (if not at the extreme boundaries of the allowed physical space) and 2) in the knots, the (infinite) quantity $\sqrt{\rho_{qm}^+(\mathbf{x})}$ $|_{x_i}$ has a positive sign, contrary to what displayed by the SQM Bohm potential in the those points. It may be referred f.i. to *Figs. 23 ÷ 27* in [2] to appreciate these features fully displayed ; there, we can think of the x_i as the positions of density minima replacing the knots.

So far, we have also demonstrated that the SQM with its linear wave equation and the non linear model can be brought to a strict neighbourhood, going through the complex plane and using generalised functions. The definitions (27), (28), (32) and (33) are, in the end, the same that in SQM but with the addition of generalised Delta corrections in the knots. To be simple but definite for further reference, we give a name to this framework, and call it the SQM⁺ model.

In the sequel we attribute the superscript (+) to all the variables specifically affected by the action of the quoted generalised functions, or specific to such context ; so f.i., we do not give the mark to the flow variable $\nu(\mathbf{x})$ and to the periods $T(E)$, because their determinations turn out independent of the Deltas being there - although we are still in the SQM⁺ frame. As an indication, an expression not marked with (+) or ($_{qm}$) can be intended for a general purpose, of use also in other contexts : notably, the NL model in its generality indeed.

4 The SQM⁺ model

The model based on the extended functions can be solved theoretically and even numerically for some typical examples. We are indeed going to show this with details.

4.1 Effective mass

We have to comply with (9) and (14). Using equations (27), (33) and (34), we have

$$m_{eff}^+(x) = \frac{c_n \hbar \rho_{qm}(x, n)^2}{8\nu(x)} + \frac{\hbar\pi \sum_{i=1}^{N_{knots}/2} \rho_{qm}^+(x_i, n) DiracDelta[x - x_i]}{2\nu(x)} \quad (38)$$

$$\int_{-\infty}^{\infty} m_{eff}^+(x) \rho_{qm}^+(x, n) dx = \int_{-\infty}^{\infty} \frac{c_n \hbar \rho_{qm}(x, n)^3}{8\nu(x)} dx + m_{knots}^+ = m \quad (39)$$

$$m_{knots}^+ = \sum_{i=1}^{N_{knots}/2} \frac{\hbar\pi \rho_i^{+2}}{2\nu(x_i)} = \frac{\hbar\pi}{2\nu_{n0}} \sum_{i=1}^{N_{knots}/2} \rho_i^{+2} = \sum_{i=1}^{N_{knots}} m_{ith\ knot}^+ \quad (40)$$

Eq. (38) means that the effective mass is a generalised function with Deltas; so this (per particle) mass is distributed in space according to a continuous part everywhere, and a part concentrated in the knots. Clearly, the expression (18) found in previous papers must reduce now to a DiracDelta so it cannot be useful here without further elaboration; however, the space extension where $\nabla S_{qm}^+(x) \neq 0$ is null so we put this task apart for now. Using the normalisation condition (14), we are able to calculate the part m_{knots}^+ anyway. This will be shown in a next section reporting the numerical calculations we have developed for the primary example of HO. Here we keep on giving other theoretical elements necessary to congruence and completeness. To this end, we have to add a few subsections herewith.

Due to the very specific considerations worth to be made as to the numerical flow $\nu(x)$ practical definition, we let this topic be the last in this section. The following arguments can indeed be understood, keeping in mind for the moment that $\nu(x)$ is a simple function conceptually : it is a constant value ν_{n0} in the oscillator's core (Regs. I and IIa), up to a position x_n . There it starts with decaying, due to particles being reflected in the boundary region (Region IIb, see f.i. fig. 32 in [2], and Fig.4 in this paper).

4.2 Group velocity

This quantity turns out now into the expression

$$v_D^+(\mathbf{x}) = \frac{2\nu(\mathbf{x})}{\rho_{qm}^+(\mathbf{x})} \quad (41)$$

We can since now appreciate its behaviour : it evanesces in the far Region II_b because the flow goes to zero there faster than $\rho_{qm}^+(\mathbf{x})$; it grows up to infinity when a knot position is approached (all the knots are in the region of space where the flow is a constant), but it takes a finite value right in the knot position

$$v_D^+(\mathbf{x}_i) = \frac{2\nu_{n0}}{\rho_i^+} \quad (42)$$

This can be seen as some hard shock occurring at the knot : in a very short time, the particle accelerates towards the knot, it dumps suddenly to a finite velocity there, and suddenly is (infinitely) reaccelerated again to the other side. Numerical data and further discussion are in the dedicated section. We may think therefore, that we need a relativistic treatment ; but this is outside of our scopes here. Yet also note, when we calculate the impulse $m_{eff}^+(\mathbf{x})v_D^+(\mathbf{x})$:

$$m_{eff}^+(\mathbf{x})v_D^+(\mathbf{x}) = \frac{c_n \hbar \rho_{qm}(\mathbf{x}, n)}{4} + \hbar \pi \sum_{i=1}^{N_{knots}/2} DiracDelta[\mathbf{x}-\mathbf{x}_i] \quad (43)$$

This last shows just the contrary behaviour : it goes to zero approaching the knot, and suddenly grows to an infinite Delta in it. So due to the mass effect, this shock shows very peculiar characters in the different lights of kinematics or dynamics (with mass effect).

4.3 Velocity fields

The velocity fields underlying quantum densities can be calculated by the same equations used in previous papers. Yet now, Region I ($\nabla S \neq 0$) reduces to the null extension of the knots positions. As a matter of fact, following our previous definitions, all the space domain here can be represented as a Region II ($\nabla S = 0$), except the knots positions placed in the extra small Reg. I. We have only to take care that "inside" the

oscillator ($|x| \leq x_n$, Reg. I+Reg. II_a), $\nu(x) = \nu_{n0}$ is a constant even with $\nabla S = 0$. We have therefore :

$$\frac{1}{2}m_{eff}^+(x)v^+(x, E)^2 = E - E_{nf} + c_n \hbar \nu(x) + \frac{\nabla S_{qm}^{+2}(x)}{2m_{eff}^+(x)} \quad (44)$$

Using previous equations we have (⁷) :

$$\begin{aligned} \frac{1}{2}m_{eff}^+(x)v^+(x, E)^2 &= E - E_{nf} + c_n \hbar \nu(x) \\ &+ \frac{\hbar \nu_{n0} \pi \sum_{i=1}^{N_{knots}/2} DiracDelta[x-x_i]}{\rho_i^+} \end{aligned} \quad (45)$$

and

$$\begin{aligned} v^+(x, E) &= \frac{4\nu(x)}{\rho_{qm}^+(x, n)} \sqrt{1 + \frac{E - E_{nf}}{c_n \hbar \nu(x)}} \left[1 - \sum_{i=1}^{N_{knots}/2} DiscreteDelta[x-x_i] \right] \\ &+ \frac{2\nu_{n0}}{\rho_i^+} \sum_{i=1}^{N_{knots}/2} DiscreteDelta[x - x_i] \end{aligned} \quad (46)$$

This leads to the following expressions for the densities included in the ensemble ($E_{ni} \leq E \leq E_{nf}$) :

$$\begin{aligned} \rho_{cl}(x, E) &= \frac{2}{T(E)v(x, E)} \rightarrow \\ \rho_{cl}^+(x, E) &= \frac{\rho_{qm}(x, n)}{2T(E)\nu(x)} \sqrt{\frac{c_n \hbar \nu(x)}{c_n \hbar \nu(x) + E - E_{nf}}} + \\ &+ \frac{\rho_i^+}{T(E)\nu_{n0}} \sum_{i=1}^{N_{knots}/2} DiscreteDelta[x-x_i] \end{aligned} \quad (47)$$

Their statistical average turns out to be (as expected ; see eq. (18) in [1] for the probability definition) :

⁷In these calculations, take into a practical account the values of each Delta in the various positions or regions of space. F.i. note that one can write for every finite quantity $w : 1/(1 + w DiracDelta[x-x_i]) =$

$(1 - DiscreteDelta[x-x_i])$. We can also write $\rho_{qm}(x, n)(1 - DiscreteDelta[x-x_i]) = \rho_{qm}(x, n)$ because $\rho_{qm}(x_i, n) = 0$.

$$\begin{aligned}
\langle \rho_{cl}^+(x, E) \rangle &= \frac{1}{c_n \hbar} \int_{E_{n,f} - c_n \hbar \nu(x)}^{E_{n,f}} T(E) \rho_{cl}^+(x, E) dE = \\
&= \rho_{qm}(x, n) + \rho_i^+ \text{DiscreteDelta}[x - x_i] = \rho_{qm}^+(x, n) \quad (48)
\end{aligned}$$

Obviously we have used

$$\begin{aligned}
T(E) &= \oint \frac{dx}{v^+(x, E)} = \\
&= \int_{-x_{0n}(E)}^{x_{0n}(E)} \frac{\rho_{qm}(x, n)}{2\nu(x)} \sqrt{\frac{c_n \hbar \nu(x)}{c_n \hbar \nu(x) + E - E_{n,f}}} dx \quad (49)
\end{aligned}$$

In these equations, $T(E)$ are the periods corresponding to each energy, calculated by classical mechanics (the contributions of the *DiscreteDeltas* in Reg. I are 0; $x_{0n}(E)$ are the turning points positions for every E value; $E_{n,f} - E_{n,i} = c_n \hbar \nu_{n0}$). By double integration, we can also easily check the norm condition

$$\begin{aligned}
&\frac{1}{c_n \hbar} \int_{E_{n,i}}^{E_{n,f}} T(E) dE = \\
&= \frac{1}{c_n \hbar} \int_{-x_0^*}^{x_0^*} \frac{\rho_{qm}(x, n)}{2\nu(x)} \left\{ \int_{E_{n,f} - c_n \hbar \nu(x)}^{E_{n,f}} \sqrt{\frac{c_n \hbar \nu(x)}{c_n \hbar \nu(x) + E - E_{n,f}}} dE \right\} dx = \\
&= \int_{-x_0^*}^{x_0^*} \rho_{qm}(x, n) dx = 1 \quad (50)
\end{aligned}$$

4.4 Energy values

We write the energy values of the n th quantum state as

$$\begin{aligned}
\langle E \rangle &= \frac{1}{c_n \hbar} \int_{E_{n,i}}^{E_{n,f}} T(E) E dE = \\
&= \frac{1}{c_n \hbar} \int_{-x_0^*}^{x_0^*} \frac{\rho_{qm}^+(x, n)}{2\nu(x)} \left\{ \int_{E_{n,f} - c_n \hbar \nu(x)}^{E_{n,f}} \sqrt{\frac{c_n \hbar \nu(x)}{c_n \hbar \nu(x) + E - E_{n,f}}} E dE \right\} dx = \\
&= E_{n,f} - \frac{2}{3} c_n \hbar \int_{-x_0^*}^{x_0^*} \rho_{qm}(x, n) \nu(x) dx = E_n \quad (51)
\end{aligned}$$

As advertised, in order to satisfy this equation - thus complying with the known SQM values E_n - we have to find a "good function" $\nu(x)$. This is done in the next section.

4.5 Numerical flow in Region II

The flow $\nu(x)$ is a constant ν_{n0} in the regions of space (I and II_a) where no reflection occurs, and the packet proceeds as a compact. Turning points are met with, instead, in the "external" region of space (II_b). We determined the boundary within these regions at the abscissas $\pm x_n$ [1], being the positions of the absolute maxima of the SQM density $\rho_{qm}(x, n)$. Correct modelling of the flow in the evanescence region is important not only to numerical calculations purposes, but also to have physical insight into the effective potential acting in this region. From eq. (44) indeed, we see that since $\nabla S_{qm}^+ = 0$ in Region II, the confinement potential is $E_{nf} - c_n \hbar \nu(x)$ - but still we need a clear glance about the physical cause of the flow variations in this zone : indeed the classical potential $\Phi(x)$ does not appear in (44), being totally screened out by the Bohm potential as is clear from eq. (4). Yet clearly, the effect depends on the quantum wave exhaustion near the border, and we could get it in a previous paper (eq. (66) in [11]) by assuming a second solution of the wave equation interpreted in the kinetic energy domain. But there, only the asymptotic behaviour was determined, while some functions (eq. (81) in [11]⁽⁸⁾) could not be determined by the procedure.

By some physical feeling however, in a following paper we could find a rather specific expression for the flow (eq. (33) in [1]) along the entire Reg. II. Actually in that paper, the entire dynamical problem governed by the variable current assumption has been solved already. Yet here, we have to go deep into this matter because the present context represents the limiting case, so strictly adjacent to the SQM one.

So first of all, trying to comply with eq. (51), we have performed numerical calculations for the HO example, using the same $\nu(x)$ expression quoted in [1]. Although this one was found effective in that context, we find now that it does not fit well in the present case, without some correction applied.

Our numerical trials indicate indeed that the effective function to be used in SQM⁺ decays faster, in the evanescence region, than allowed by the old position. So we came to another level of analysis, i.e. to a thermodynamical model of the quantum fluid in the space domain.

⁸In [11], the so called Reg. I is actually part of what we have called Reg. II in subsequent papers.

This last cannot take place here, and we reserve it to a next paper. But as far as we are concerned now, giving only a few basic elements will be enough to find out more effective modelling for $\nu(\mathbf{x})$.

In eqs. (35)÷(38) of ref. [1] we met with the quantity - give it a name $\langle K'_{th} \rangle$:

$$\langle K'_{th} \rangle = \frac{c_n^2 h^2 \rho(\mathbf{x})^2}{32m_{eff}(\mathbf{x})} \quad (52)$$

This quantity takes its place in the classical energy theorem describing the ensemble with effective mass $m_{eff}(\mathbf{x})$. We attributed to it, in Region I, the role of a kinetic energy "inside the packet", i.e. an energy in the reference frame travelling with velocity v_D . Note yet, that this expression may not everywhere be exhaustive of the kinetic energy in that frame : indeed some other fraction may come from the other potentials in the balance (this certainly occurs in Region II_b, when the probability distribution $P(E)$ is not a constant across the energy domain.

Notwithstanding, it is a very peculiar potential to the system. Indeed, it fully plays its role of internal energy in Reg. I (eq. (38) in [1]), while in Reg. II we found that it shares exactly the same amount of energy with the translational degree of freedom (eq. (45) in [1], with $E_p = 0$).

So we attempt here the interpretation that it is an exchangeable energy, contained in 1 definite (kinetic) degree of freedom. In practice, we assume that it is the thermodynamic energy (actually, the temperature-dependent part of it, say $U(T)$). See next note ⁽⁹⁾). Contextually, we also assume a constant volume specific heat of 1/2 (Boltzmann's $k_B = 1$). This brings us to a thermodynamic model where the temperature field is

$$T(\mathbf{x}) = \frac{U(T)}{c_V} = \frac{c_n^2 h^2 \rho(\mathbf{x})^2}{16 m_{eff}(\mathbf{x})} \quad (53)$$

c_V being taken

$$c_V = \frac{1}{2} \quad (54)$$

everywhere.

By this way, in the easy assumption of a perfect gas ⁽⁹⁾, the main consequences here are : first, that in Region II_a the transformation $T(\rho)$

⁹It is *not exactly* a perfect gas. It can be shown by eq. (37) in [1] that a small part of the internal energy depends on the volume $1/\rho$ in Region II_b. But one will also find that this only affects work and heat functions, not the enthalpy. So for the simple considerations here, this detail can be neglected. Deeper analysis is to come in a next paper.

is an isothermic; and second, it cannot be an isentropic in Region II_b because this would require ⁽¹⁰⁾

$$\frac{c_n h \nu(\mathbf{x})}{2} = T(\mathbf{x}) \propto \rho(\mathbf{x})^2 \quad \{\text{Reg. II}_b\} \quad (55)$$

while in the far Reg. II_b we have instead

$$\nu(\mathbf{x}) \rightarrow \sqrt{\frac{\mu_n}{2m}} \rho(\mathbf{x})^{\frac{5}{4}} \quad (56)$$

In the asymptotic region towards the border, indeed, we have found a 5/4 power law in previous work. All of this means that the transformation in Reg. II_b is a sort of polytropic : we can simulate it f.i. by

$$\frac{c_n h \nu(\mathbf{x})}{2} = T(\mathbf{x}) \propto \left(\frac{\rho(\mathbf{x})}{\rho(\mathbf{x}_n)} \right)^{\frac{5}{4} + \theta \frac{\rho(\mathbf{x})}{\rho(\mathbf{x}_n)}} \quad (57)$$

The flow function behaviour can therefore be identified in this equation. Clearly, we have taken an easy form for the (variable) exponent in expression (57). Inserting the last in eq. (51), we can find by numerical calculus, for each oscillator and level at hand, the value of the constant θ complying with each required E_n value. As is shown in *Fig. 4*, this model brings to us a fast flow decay in the boundary Region II_b (as anticipated indeed); followed by a longer evanescent tail.

Before giving the announced example, we add some other general comments here.

5 Commentaries

A thermodynamic model also implies that a pressure acts on the packet giving expansion work near the border. Yet the particles group is decelerated while approaching the walls. According to eq. (37) in [1] indeed, expansion accompanies with decreasing, towards boundary, of all

¹⁰The purely classical ensemble investigated in [11], f.i., complies with eq. (55). This is just because the distribution $P(E)$ was assumed a constant in that work. It is useful here to recall that in our models, the quantum ensemble differs from the classical one just by the addition of 2 ingredients more in the energy theorem : the quantum potential (eq. (61) in [1]) including the mass effect; and the energy distribution $P(E)$ taken proportional to the periods $T(E)$. Note that microfluidic systems with a linear coupling between velocity and density are known [12], and obviously a variety of other behaviours are also found discussed in the literature [13,14].

the other pilot quantities (temperature, energy broadening $c_n h \nu(x)$ and flow (this defines the reactive potential k_{VMRE} in [1]).

Taking all of these effects into account from the point of view of the equivalent single particle with velocity $v_D(x)$ and regular mass m , we can write from eq. (9) (everywhere; the expression is a general one, but let us discuss it with reference to the SQM⁺ model) :

$$\frac{1}{2}m v_D^+(x)^2 - m \frac{c_n h \nu(x)}{4m_{eff}^+(x)} - \frac{m \nabla S_{qm}^{+2}(x)}{2m_{eff}^{+2}(x)} = 0 \quad (58)$$

This means that in Region II_b the equivalent classical particle has to climb up the potential $-mc_n h \nu(x)/4m_{eff}^+(x)$, as is clear on a general plane from previous work already. The asymptotic expression towards the border given by this equation for $v_D(x)$ is $\propto \rho(x)^{\frac{1}{4}}$ as it must. From the point of view of the particle with perturbed mass, the potential to go up is simply $-c_n h \nu(x)/4$, i.e. 1/4 of the characteristic energy broadening of the system. One can show that the remaining 3/4 of this same energy are balanced with enthalpy pertaining to the travelling particles packet. The balance of all these potentials accounts for deceleration and exhaustion of the packet at the far border.

The same potential forms (but with constant flow) hold all along in Region II_a. Near the knots, $m_{eff}^+(x) \rightarrow 0$ so that $v_D^+(x) \rightarrow \infty$ but *in* the knots (Region I), the generalised values $-\nabla S_{qm}^{+2}(x_i)m/2m_{eff}^{+2}(x_i)$ stay for slim peaks of negative potential. The particle has an infinite velocity when it meets with them; as said already, we can think of this situation as of a very hard shock reporting the particle to cross the knot with finite velocity $v_D^+(x_i)$. It is interesting that at same time in the knot, the wave phase shows a sudden infinite step, while the temperature suddenly falls down to zero (due to the infinite mass $m_{eff}^+(x_i)$). In the knot, the particle only brings wave momentum, with no internal motion accompanying it in the packet : this slims to zero depth quickly.

This last fact can also be seen from the detailed energy theorem : (44) shows us, with some easy definitions (but take a general view, use (9) and (11)) :

$$u(x) = v(x, E) - v_D(x) \quad (59)$$

$$v_{\max}(x) \equiv v_f(x) = v(x, E_{nf}) = \sqrt{\frac{2c_n h \nu(x)}{m_{eff}(x)} + \frac{\nabla S^2(x)}{m_{eff}(x)^2}} = u_{\max}(x) + v_D(x) \quad (60)$$

$$v_{\min}(x) \equiv v_i(x) = v(x, E_{nf} - c_n h \nu(x)) = \frac{\nabla S(x)}{m_{eff}(x)} = u_{\min}(x) + v_D(x) \quad (61)$$

$$\frac{v_{\max}(x) + v_{\min}(x)}{2} = v_D(x) \quad (62)$$

$$v_{\max}(x) - v_{\min}(x) = 2(v_{\max}(x) - v_D(x)) = 2u_{\max}(x) = \frac{c_n h \rho(x)}{2m_{eff}(x)} \quad (63)$$

The last expression evaluates the interval of velocities included in the packet and the maximum relative velocity $u_{\max}(x)$ with respect to $v_D(x)$. It also defines the $U(T)$ value as ⁽¹¹⁾

$$U(T) = \frac{1}{2} m_{eff}(x) \left\{ \langle u^2(x) \rangle + 2 \langle u(x) \rangle v_D(x) \right\} = \frac{1}{2} m_{eff}(x) u_{\max}^2(x) \quad (64)$$

So when in SQM⁺ $m_{eff}(x) \rightarrow m_{eff}^+(x_i) \rightarrow \infty$ in a knot, the velocities packet reduces to the single-valued ensemble

$$v^+(x_i, E) = v_D^+(x_i) \quad (65)$$

A detailed thermodynamic model can be developed, not only for the space regions here considered in the SQM⁺ case, but also for the Region I in the general case of distributed ∇S as in [1,2]. As advertised however, we leave all of this to a next article. On a general plane, eqs. (60)÷(62) still deserve the following comment here.

In the particles ensemble view, those equations just identify the packet extension in the momenta space at the position x . When we assume instead, by ergodicity, that a single particle runs over the interval $v_{\max}(x) - v_{\min}(x)$ - yet "staying" in the position x - we have to admit that this motion is extraordinarily fast in comparison with the time scale related to the same v_D . It is useful to recall here that at the origin of our model is the Kapitza theorem, distinguishing between different scales of velocities fluctuations. Therefore, we understand that another very fast scale of motions is hidden in our context beyond what investigated here. The arithmetical mean displayed in (62) can be interpreted indeed, as if the particle is submitted to an infinite impulse of constant acceleration between x and $x+dx$, and suddenly back in the following space and time intervals dx, dt . In the same time, on a slower time scale, the drift v_D is

¹¹By its definition, $v_D(x)$ is a "group" velocity so it may not be coincident with the center of mass velocity calculated in x .

effective. So the assumption of a many, infinite impulses train spectrum across the time indicates the occurrence of very fast velocity fluctuations seeming to us very much alike the known *Zitterbewegung* motions first supposed by Schrodinger and Dirac. Then with our models, we are actually investigating a slower part of the quantum motions; but as a matter of fact to our belief, it seems well that we are able to give an interesting model on this scale already.

We are now going to give numerical results for the primary example of the harmonic oscillator. They are best expressed into next tables and figures; a few other commentaries are included thereabout.

6 Numerical example : the Harmonic Oscillator

The normalised quantum density (33) for HO writes, as a function of $\xi = x/\lambda$ ($N_{knots} = 2(n-1)$) :

$$\rho_{qm}^+(\xi, n) = \rho_{qm}(\xi, n) + \rho_1^+ \sum_{i=1}^{N_{knots}/2} DiscreteDelta[\xi - \xi_i] \quad (66)$$

The effective mass function (38) is

$$m_{eff}^+(\xi) = \frac{c_n \hbar \rho_{qm}(\xi, n)^2}{8 \nu(x)} + \frac{\hbar \pi \rho_1^+}{2 \lambda \nu_{n0}} \sum_{i=1}^{N_{knots}/2} DiracDelta[\xi - \xi_i] \quad (67)$$

By normalisation (39) we have therefore

$$\int_{-\infty}^{\infty} m_{eff}^+(\xi) \rho_{qm}^+(\xi, n) dx = \int_{-\infty}^{\infty} \frac{c_n \hbar \rho_{qm}(\xi, n)^3}{8 \nu(x)} dx + \frac{\hbar \pi \rho_1^{+2}}{4 \nu_{n0}} N_{knots} = m \quad (68)$$

$$m_{knots}^+ = m - \frac{c_n \hbar \lambda}{8} \int_{-\infty}^{\infty} \frac{\rho_{qm}(\xi, n)^3}{\nu(x)} d\xi = \frac{\hbar \pi \rho_1^{+2}}{4 \nu_{n0}} N_{knots} \quad (69)$$

In these equations, still $\nu(\xi)$ and ρ_1^+ are unknown values, but we can find $\nu(\xi)$ from eq. (57) assuming the good value of θ able to satisfy eq. (51); once $\nu(\xi)$ is known, we can find ρ_1^+ and m_{knots}^+ from (69). So we have (give a mark n to ν) :

$$\nu_n(\xi) = \nu_{n0} UnitStep[\xi_n - \xi] +$$

$$+\nu_{n0} \text{UnitStep}[\xi - \xi_n] \left(\frac{\rho_{qm}(\xi, n)}{\rho_{qm}(\xi_3, n)} \right)^{\frac{5}{4} + \theta_n \frac{\rho_{qm}(\xi, n)}{\rho_{qm}(\xi_n, n)}} \quad (70)$$

$$E_n = \left(n - \frac{1}{2} \right) h\nu_c = E_{nf} - \frac{1}{2} h\nu_c \quad (71)$$

$$\nu_{n0} = \frac{\nu_c}{c_n} \quad (72)$$

Eq. (51) writes therefore

$$\text{UnitStep}[\xi_n - \xi] \int_0^\infty \frac{\rho_{qm}(\xi, n)}{\rho_{qm}(\xi_n, n)} d\xi + \quad (73)$$

$$+\text{UnitStep}[\xi - \xi_i] \int_0^\infty \left(\frac{\rho_{qm}(\xi, n)}{\rho_{qm}(\xi_n, n)} \right)^{\frac{9}{4} + \theta_n \frac{\rho_{qm}(\xi, n)}{\rho_{qm}(\xi_n, n)}} d\xi =$$

$$= \frac{3}{8 \lambda \rho_{qm}(\xi_n, n)} \quad (74)$$

This can also be written

$$I_{n1} = \int_0^\infty \left(\frac{\rho_{qm}(\xi, n)}{\rho_{qm}(\xi_n, n)} \right)^{\gamma(\xi)} d\xi = \frac{3}{8 \lambda \rho_{qm}(\xi_n, n)} \quad (75)$$

$$\gamma(\xi) = \text{UnitStep}[\xi_n - \xi] + \left(\frac{9}{4} + \theta_n \frac{\rho_{qm}(\xi, n)}{\rho_{qm}(\xi_n, n)} \right) \text{UnitStep}[\xi - \xi_n] \quad (76)$$

and from these eqs. we can find the θ_n values.

Once this task accomplished, $\nu_n(\xi)/\nu_{n0}$ is known (it is a quantity depending only on the qm wavefunction at hand). So let us write eq. (69) as

$$m_{knots}^+ = m(1 - c_n^2 I_{n2}) = \frac{c_n h \rho_1^{+2}}{8\nu_c} N_{knots} = m_{ith\ knot}^+ N_{knots} \quad (77)$$

$$I_{n2} = \pi^2 \lambda^3 \nu_{n0} \int_0^\infty \frac{\rho_{qm}(\xi, n)^3}{\nu_n(x)} d\xi \quad (78)$$

and we have

$$\rho_1^+ = \sqrt{\frac{8m\nu_c}{c_n h N_{knots}} (1 - c_n^2 I_{n2})} \quad (79)$$

In these equations, only c_n is an unknown parameter now. In previous work, the c_n values were determined by the imposed constraints to ∇S and the $m_{eff}(x)$ but they were regular functions in a non-zero domain there, so we cannot use the same techniques now. Actually, we do not have available an *exact* condition to impose here, but we can have an approximate view just referring to that previous work. Indeed when each of the peaked $\nabla S_{qm}^+(x_i)$ broadens into a more regular bell shape, its width should be of the order of $\xi_n \lambda / N_{knots}$ so that we can estimate the mass statistically stored in a knot to be of the order of

$$\frac{m_{knots}^+}{N_{knots}} = \frac{\hbar \pi \rho_1^{+2}}{4\nu_{n0}} \approx \frac{\xi_n \lambda \rho_1^+ m}{N_{knots}} \rightarrow \quad (80)$$

$$\rightarrow c_n(1 - c_n^2 I_{n2}) \approx 8\xi_n^2 \lambda^2 \frac{m\nu_c}{\hbar N_{knots}} \quad (81)$$

From this equation, we obtain indeed values of c_n (shown in Table I) which are, for the first few levels (2 ÷ 5) of HO, not far from those obtained in [2]. These first-levels values of the quantities I_{n1} , I_{n2} , c_n and other ones can all be found in Table I. For levels with $n > 5$ eq. (81) gives a series of decreasing c_n values towards 0, which are instead not in agreement with the results in [2]. All of these and next issues will be found better discussed in the next dedicated section. Now using just the values of Table I we plot some representatives of the other functions of interest, for a few sampled values of n , in *Figs. 3 ÷ 10*.

n	1	2	3	4	5	6	7
N_{knots}	0	2	4	6	8	10	12
I_{n1}	0.6647	0.9034	1.0122	1.0850	1.1405	1.1857	1.2239
I_{n2}	1.0516	0.6659	0.5841	0.6197	0.8197	1.5320	5.1373
c_n	0.9752	1.1712	1.2399	1.1937	1.0213	0.7158	0.3069
m_{knots}^+ / m	0.0865	0.1022	0.1172	0.1450	0.2151	0.5160
$\lambda \rho_1^+$	0.0865	0.0646	0.0576	0.0560	0.0780	0.1685
θ_n	-0.8776	1.1455	2.9294	4.8864	7.2690	10.424	14.950
ξ_n	0	1	1.5811	2.0341	2.4177	2.7562	3.0625

Table I-numerical values for various coefficients of interest

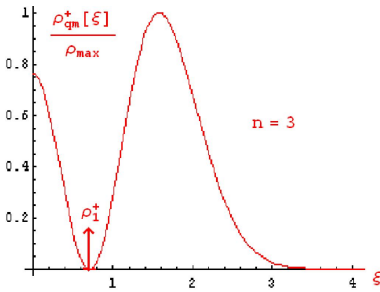


Fig. 3 -

SQM+ density for HO, $n = 3$

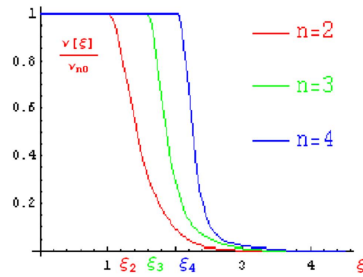


Fig. 4 -

flow functions for SQM+ HO, $n = 2, 3, 4$

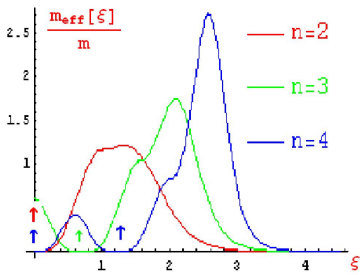


Fig. 5 -

SQM+ HO mass functions, $n = 2, 3, 4$

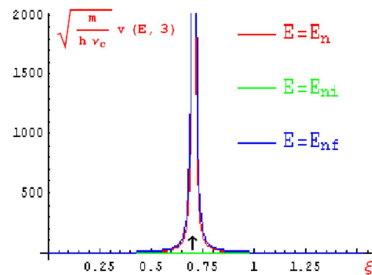


Fig. 6 -

SQM+ HO velocity fields, $n = 3, \xi \leq \xi_3$

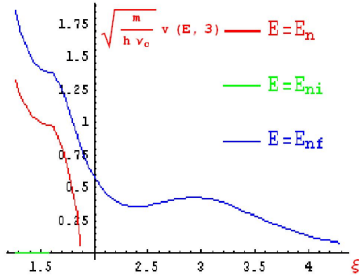


Fig. 7 -

SQM+ HO velocity fields, $n = 3, \xi > \xi_3$

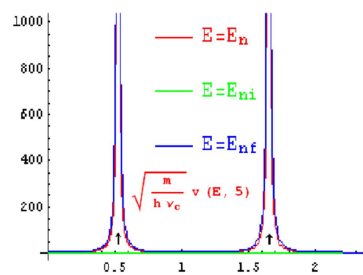


Fig. 8 -

SQM+ HO velocity fields, $n = 5, \xi \leq \xi_5$

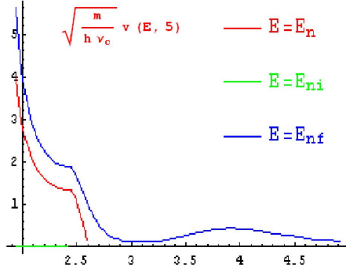


Fig.9-

SQM^+ HO velocity fields, $n=5, \xi > \xi_5$

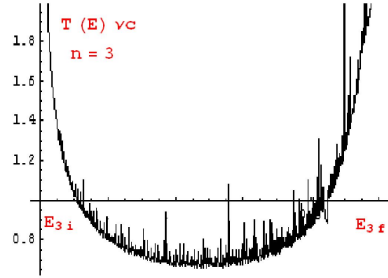


Fig.10-

periods vs energy for HO, $n=3$

In *Figs* 3, 5, 6, 8, beyond the regular curves for each variable, we duly placed the vertical arrows in the knots, representing the extra values introduced in the SQM^+ context by the generalised functions. In *Fig. 5* they stand for DiracDelta functions, while in 3, 6, 8 the arrow is simply a DiscreteDelta. It can be noted in this last that peaks of effective mass tend to move to the border where they become higher with growing n ; this behaviour is concomitant with the particles flow fast decaying in the same region, and density decreasing. We have commented already about the velocity fields near the knots, in a previous section; and in [2] from a more general point of view. Here it can be said that the behaviour of these fields with different energies in Reg. I is rather uniform (but note that at the energy E_{ni} , the velocity $v(x, E_{ni})$ is zero everywhere; the model says us that particles with minimal energy stay at rest all along Reg. I). In Reg. II instead, the fields separate quickly into different patterns, whose evolutions are much correlated to the distance of the corresponding turning points at the border. In *Fig. 9* we give a sample of periods as functions of energy in the fluctuation interval, for the case $n = 3$. Numerical integration performed (with the standard command and ordinary precision) in Wolfram Mathematica of the velocity fields brings in this plot some randomness, probably due to the exceedingly fast variations of the integrands in Reg. I and concomitant fast and irregular variations in Reg. II. However, the plot interpretes easily by the dominance of two singularities in E_{ni} and E_{nf} , where the periods become infinite (but remain integrable). In particular, the field $v(x, E_{nf})$ causes an infinitely long period since it moves up to the extreme boundary $x \rightarrow \infty$ in the HO; this is consistent with the estimate of a very small tunneling out probability in the hypothetical assumption

that the HO attractive potential is eventually broken at a far distance, letting particles flow out. Adequate to these points, other comments are also available in [3].

The trend of c_n and m_{knots}^+ towards growing values of n as shown in Table I looks consistent with the current interpretation of SQM as pointing to the classical limit with decreasing influence of the Planck constant : indeed the c_n appear as coefficients of h in our model, and when they become smaller the quantum h action is more and more screened out. At the same time, the mass concentrated in the knots grows, bringing importance to the region of space with $\nabla S \neq 0$ - this is clearly a trend towards the classical world where $\nabla S = m v_D$ in all space. Notwithstanding, the classical limit perspective offered by these features does not give us a clearer view than is not known already, about the necessity to proceed with JWKB methods. As a matter of fact, in order to insure the approach to classical world, starting with a certain n value the SQM stationary framework with real wavefunctions as in (20) must be upset in a travelling wave context. In the SQM⁺ frame as here introduced, this particular trouble disappears but as far as the Bohm potential is not deactivated in the wave equation, knots will not be removed, and the classical limit will remain quite hard to be mathematically reached or conceptually explained. Furthermore, we note by eq. (72) that realistic values of c_n cannot be very different from unity, because even in quantum mechanics the particles flow in a level cannot be very different from the classical, for great values of n at least. We are better brought to believe in a model where the c_n trend at high n 's is towards unity, than the contrary. At the same time, a distributed phase gradient along the space is appreciable, since it is able to evolve naturally towards a classical character. Obviously SQM is able to mix functions to this end - but as long as the mixing is restrained to a condition of *linearity*, it may be found that explaining the classical world in terms of the quantum one remains very laborious and (we think) technically criticizable.

7 Conclusion

Interpreting the SQM model as the linear approximation of the variable current model implies the following view. Quantum mechanics describes a resonant interaction between particles (intended in their classical nature) and quantum vacuum, this last imposing its peculiar constraints to their motion. Just as in classical resonance problems, a first step of description (here, the SQM) can be made by neglecting any broadening.

This looks like the forced classical oscillator case, when we suppress friction in the equation. Then clearly, we get the natural resonance frequency from the linearised equation : indeed SQM provides the energy eigenvalues with great effectiveness. If now some "not too big" broadening is introduced in the description, we know that for ordinary systems the consequent frequency displacement will be very small. So the linear SQM is quite the useful tool to calculate resonances with great effectiveness, explaining its overwhelming success. Introducing broadening however, brings us to the non linear model where the current density is variable and the phase gradient $\nabla S/\hbar$ distributes over the space domain, instead of being concentrated in the knots as we have seen in this paper. This view has also brought us to a peculiar interpretation of the classical limit, expounded in refs. [1,2]. By the way, that is why we did not need a priori *calculating* the energy eigenvalues there with the non linear model ; we just assumed the known values by SQM. The demonstrated very high precision of spectroscopic lines calculations with SQM might also induce us to think that in a quantum system the resonance is so strong that broadening does not change perceptibly the natural frequencies i.e. the energy eigenvalues. As far as selection rules are regarded, since they depend on the wavefunctions symmetries, one can note, f.i., that a NL travelling wave amplitude cannot show an odd symmetry in space because it takes no zeros. But the distributed phasor $Exp[iS(x)/\hbar]$ real and imaginary parts do have all the symmetry characters, so we can use them (although not so simple as in SQM) to reproduce the spectroscopic rules even in the NL model . However, the distributed phase gradient model should be considered for the sake of identifying more realistic wavefunctions and effective information about vacuum action and many physical parameters which are completely screened out in SQM ; as well as to settle paradoxes inevitably consequent to the assumption of linear superposition of waves. Amongst other in our belief, linearity is just the cause which makes us unable to escape the puzzling dilemma of the cat dead *and* alive - if not at the very moment when we open the box.

References

- [1] MASTROCINQUE G., Ann. de la Fond. L. de Broglie 36, 91 (2011)
- [2] MASTROCINQUE G., Ann. de la Fond. L. de Broglie 36, 159 (2011)
- [3] MASTROCINQUE G., http://www.fedoa.unina.it/9058/1/Comments_on...pdf

- [4] WALKER J., Sci. Am. 238 (6), 123 (1978)
- [5] COUDER Y., PROTIERE S., FORT E. and BOUDAUD A., Nature 437 (7056), 208 (2005)
- [6] PROTIERE S., BOUDAUD A. and COUDER Y., J. Fluid Mech. 554 (10), 85 (2006)
- [7] EDDI A., FORT E., MOISY F. and COUDER Y., Phys. Rev. Lett. 102 (24), 240401 (2009)
- [8] OZA A. U., ROSALES R.R. and BUSH J. W. M., J. Fluid Mech. 737, 552 (2013)
- [9] SBITNEV V. I., ArXiv :1307.6920v1 [physics.flu-dyn] (2013)
- [10] BRADY R. and ANDERSON R., ArXiv :1401.4356v1 [quant-ph] (2014)
- [11] MASTROCINQUE G., Ann. de la Fond. L. de Broglie 28, 119 (2003)
- [12] BEATUS T., TLUSTY T. and BAR-ZIV R., Phys. Rev. 103, 114502 (2009)
- [13] COCCO R., REDDY KARRY S. B. and KNOWLTON T., Introduction to fluidization, PSRI/AICHE (2014) : <http://www.aiche.org/sites/default/files/cep/20141121.pdf>
- [14] HOLDICH R. G., Fundamentals of particle technology, Loughborough University, Midland Information Technology and Publishing, Shepshed UK (2002) : http://www.particles.org.uk/particle_technology_book/particle_book.htm

(Manuscrit reçu le 10 octobre 2015)